

## Potential for atmospheric neutrino physics with JUNO

---

**Marta Colomer Molla<sup>a,\*</sup> and on behalf of the JUNO collaboration**

<sup>a</sup>*Institution,*

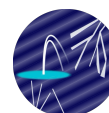
*Street number, City, Country*

<sup>b</sup>*Inter-university Institute for High Energies (IIHE), Université Libre the Bruxelles (ULB),  
Brussels, Belgium*

*E-mail:* [marta.colomer@ulb.be](mailto:marta.colomer@ulb.be)

The Jiangmen Underground Neutrino Observatory (JUNO) is a next-generation neutrino experiment located in China, currently undergoing the commissioning phase. With 20 ktons of ultra-pure Liquid Scintillator (LS), JUNO seeks to make world leading measurements of three neutrino oscillation parameters and determining the Neutrino Mass Ordering (NMO). Even though it is designed to primarily use reactor neutrinos to this aim, JUNO will also be able to study neutrino oscillations using atmospheric neutrinos, which will provide a synergetic channel exploiting matter effects on neutrino oscillations. This talk will report the latest updates on the JUNO capabilities for atmospheric neutrino detection at GeV energies.

39th International Cosmic Ray Conference (ICRC2025)  
15–24 July 2025  
Geneva, Switzerland



**ICRC 2025**

The Astroparticle Physics Conference  
Geneva July 15-24, 2025

---

\*Speaker

## 1. Introduction

The main objective of JUNO [1] is to determine neutrino mass ordering (NMO) using reactor neutrino (MeV) oscillations in vacuum [2]. The central detector of JUNO will consist of 20 kton of liquid scintillator contained in an acrylic sphere of 35 m diameter. JUNO will observe the scintillation light produced by particle interactions in the detector with  $\sim 40,000$  photomultiplier tubes ( $\sim 78\%$  coverage). JUNO is surrounded by a Cherenkov detector veto (the water pool, WP), and on top of it, the top tracker (TT) is placed to further identify vertical downwards-going muons.

Due to its big size and characteristics, JUNO will also be able to detect atmospheric neutrinos produced in cosmic ray interactions in the atmosphere. Indeed, atmospheric neutrinos and antineutrinos of a wide range of energies travel through the Earth with various path lengths, providing sensitivity to NMO via matter effects on neutrino oscillations, thus providing a complementary channel for JUNO to study neutrino oscillations and the NMO. The NMO measurement in this case is driven by an expected hierarchy-dependent, upward-going excess of either electron neutrino or antineutrino interactions due to matter effects between 2 and 10 GeV [3]. This can be seen in the oscillation probability ( $\nu_e \rightarrow \nu_e$ ) distributions drawn in Figure 1. Matter effects on neutrino oscillations will therefore depend on the energy and incident angle of the neutrino (zenith angle), as well as on neutrino type (flavor). Moreover, while neutrinos will experience matter effects in the case of normal ordering, the same effect will be observed in anti-neutrino if the mass ordering is inverted. As JUNO is not originally designed for GeV physics, it is thus crucial to evaluate the detector response to neutrino interactions in this energy range. In the following sections, the JUNO capabilities for energy and direction reconstruction, as well as for separating the different neutrino types (particle identification) will be presented.

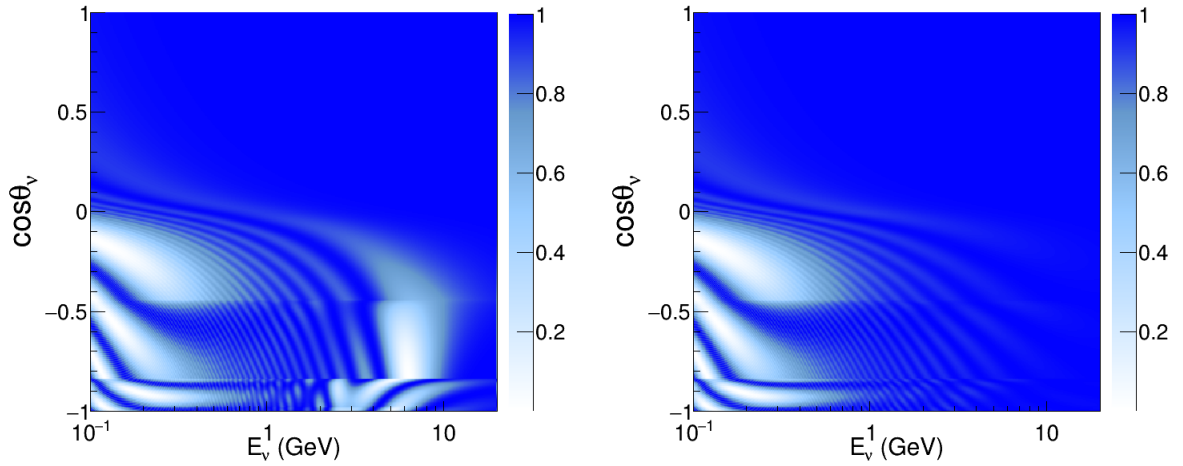


**Figure 1:** Electron neutrino oscillation probabilities ( $\nu_e \rightarrow \nu_e$ ) as a function of the zenith angle and the neutrino energy, for each neutrino mass ordering scenario (normal on the left, inverted in the right).

## 2. Expected number of events

We estimate the true number of charged-current (CC) and neutral-current (NC) interactions of atmospheric neutrino events in the liquid scintillator (LS) of the JUNO central detector. The number of CC interactions of atmospheric neutrinos of flavor ( $\nu_\alpha$ ), in the neutrino energy bin  $i$  ranging from  $E_{min}^i$  to  $E_{max}^i$  and the cosine of the neutrino direction bin  $j$  in the range from  $\cos \theta_{min}^j$  to  $\cos \theta_{max}^j$  without neutrino flavor oscillations is given by:

$$N_{ij}^{\nu_\alpha, CC} = 2\pi N_t \int_{\cos \theta_j^{min}}^{\cos \theta_j^{max}} d(\cos \theta) \int_{E_i^{min}}^{E_i^{max}} dE \sigma_{\nu_\alpha}^{CC}(E) \sum_{\nu_\beta} \frac{d^2 \Phi_{\nu_\beta}}{d \cos \theta dE} P_{\nu_\beta \rightarrow \nu_\alpha}(E, \cos \theta) , \quad (1)$$

with

$$N_t = T \times N_A \times M_{det} . \quad (2)$$

Here,  $N_A$  denotes the Avogadro number (/mole),  $T$  is the exposure time in seconds, and  $M_{det}$  represents the detector mass (= 20 kton). The CC interaction cross sections of GeV neutrinos (of flavor  $\alpha$ ) are produced by the neutrino generators with the targets  $^{12}C$  ( $\sigma_C^\alpha$ ) and  $^1H$  ( $\sigma_H^\alpha$ ) in the units of  $m^2/\text{nucleons}$  which are then weighted by the fraction of hydrogen ( $f_H$ ) and carbon ( $f_C$ ) and their molar masses ( $M_H$  and  $M_C$ ) to get  $\sigma_{\nu_\alpha}^{CC}$ ,

$$\sigma_{\nu_\alpha}^{CC} = \frac{f_H \times \sigma_H^\alpha}{M_H} + \frac{f_C \times \sigma_C^\alpha}{M_C} . \quad (3)$$

For the neutrino fluxes, we consider their differential forms ( $\frac{d^2 \Phi_{\nu_\alpha}}{d \cos \theta dE}$ ) as the functions of  $\cos \theta$  and energy in the units of  $m^{-2} \text{ sec}^{-1} \text{ sr}^{-1} \text{ GeV}^{-1}$ , as provided by the Honda et.al. We interpolate these fluxes at any energies and directions using a 2-dimensional spline-based interpolation. The factor  $2\pi$  in front of the Eq.?? appears from the integration over azimuthal angle of the flux since we consider the averaged fluxes over it. The cross-sections ( $\sigma_{\nu_\alpha}^{CC}$ ) are calculation using the GENIE generator [4]. The number of NC interactions of atmospheric neutrinos is obtained by replacing the cross section for the CC interaction by the NC interaction ( $\sigma_{\nu_\alpha}^{NC}$ ) in Eq. ??, and it is summed over all neutrino flavors. Finally,  $P_{\nu_\beta \rightarrow \nu_\alpha}(E, \cos \theta)$  denotes the probability of neutrino  $\nu_\beta$  changing to ( $\beta \neq \alpha$ ) or surviving as ( $\beta = \alpha$ )  $\nu_\alpha$ . The antineutrino ( $\bar{\nu}$ ) events are estimated with Eqs. ?? and 1 by changing  $\nu \rightarrow \bar{\nu}$ . In the context of atmospheric  $\nu$  and  $\bar{\nu}$ , only electron and muon flavors are produced in the interactions of primary cosmic particles in the atmosphere of Earth. Therefore, the subscripts  $\beta \in [e, \mu]$ .

With that, one can estimate that the expected number of atmospheric neutrino events in JUNO within six years of data taking is of  $\sim 19100$  in total,  $\sim 7500$  being neutral current interactions (NC), which are part of the background as they are not sensitive to matter effects), and  $\sim 3700$  are  $\nu_e$ -CC, which will give the dominant NMO signal. This is dependent on the interaction models, and subject to uncertainties on the atmospheric neutrino flux.

## 3. Event selection

The main background for atmospheric neutrino analyses in JUNO are cosmic muons. Located  $\sim 650$  m underground to mitigate to comic muon impact, the expected rate in the JUNO central

detector is of  $\sim 5$  Hz. In contrast, only  $\sim 10$  atmospheric neutrino interactions are expected per day. The two veto detectors described before (TT and WP) will allow us to tag muons with  $>99\%$  efficiency. While neutrino interactions happen inside the detector (most of them are fully contained, FC, events), muons enter the detector after traversing the rock. Moreover, neutrinos can traverse the Earth and reach the detector, they will come from below the horizon, upwards-going, while muons will be coming only from above, downwards-going, as they can't cross the Earth before being absorbed/decaying. These two features will allow to further remove the remaining muons, and keep the background to a negligible level in the region where matter effects occur.

#### 4. Direction and energy reconstruction

The directionality information of incoming neutrinos is essential to atmospheric neutrino oscillation analyses since it is directly related to the oscillation baseline length. Homogeneous liquid scintillator detectors, while offering excellent energy resolution, are traditionally very limited in their capabilities of measuring event directionality. However, with the information extracted from the PMT waveforms and its large size and PMT coverage, JUNO can exploit the pattern of the scintillation light seen across the detector to get direction information.

Using these PMT waveform features (first hit time, total and maximum charge, slope) as input to a machine learning (ML) algorithm, JUNO may achieve a good direction resolution and potentially play an important role in future atmospheric neutrino oscillation measurements, as demonstrated in [5]. The results, shown in Figure 2, show that the angular resolution is  $<10^\circ$  for neutrino energies above 3 GeV (i.e. in the NMO region).

The same machine learning model can be trained (with the same PMT feature information as input) to reconstruct the neutrino energy. The difficulty for that is that, while JUNO is very good at reconstructed the visible energy, in atmospheric neutrino interactions, part of the energy goes to invisible energy, or is deposited outside of the detector. Thus, the relation between the visible and the neutrino energy is not trivial, and it is dependent on the interaction models. Figure 3 shows the energy resolution result, which is below 10%, both for electron and muon neutrinos (charged current interactions), in the energy range of interest.

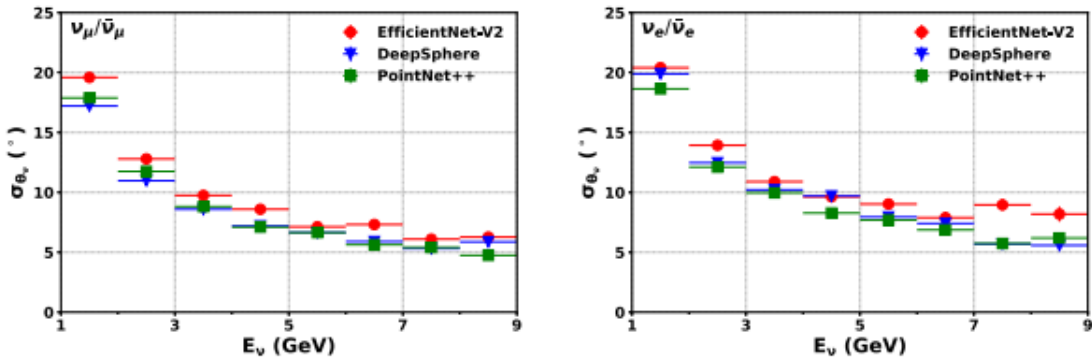


**Figure 2:** Uncertainty on the reconstructed zenith angle ( $\theta$ ) as a function of the true neutrino energy, using three different machine learning models. Figure extracted from [5], where more details about the ML methods and architecture can be found.

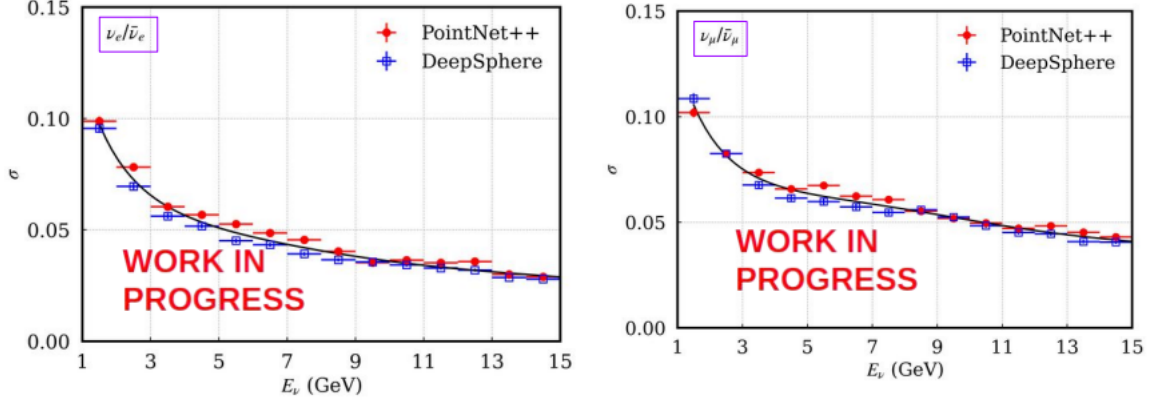


**Figure 3:** Uncertainty on the reconstructed neutrino energy as a function of the true neutrino energy, using two different machine learning models.

## 5. Neutrino type identification (PID)

The atmospheric neutrino flux is a mixture of muon (anti)neutrino ( $\nu_\mu/\bar{\nu}_\mu$ ) and electron ( $\nu_e/\bar{\nu}_e$ ) and hence the neutrino flavor needs to be identified in the detector to identify changes in the oscillation probabilities. Moreover, the ability to identify neutrinos against antineutrinos is important since matter effects distort their oscillation probability in opposite ways, as mentioned before. While experiments lacking such capability still get some sensitivity to NMO from small differences in fluxes and cross sections for neutrinos and antineutrinos, the discriminating power between the neutrinos and antineutrinos certainly helps to disentangle NMO and CP violation phase and increase the sensitivity. However, such flavor identification and neutrino/antineutrino discrimination have never been achieved in LS detectors before.

Using the full JUNO monte-carlo simulation, the PID capabilities of JUNO have been studied. Indeed, as for the direction, the scintillation light pattern encodes information on the topology and features of the interaction, giving access to the neutrino type. The results in [6] suggest that JUNO will have an unprecedented performance in this regard compared to other atmospheric neutrino experiments. The PID can be divided into two steps. First, separating charged and neutral current interactions together with the neutrino type into three classes ( $\nu_\mu$ -CC,  $\nu_e$ -CC, and NC). Then, separating neutrinos from anti-neutrinos, for each flavor individually. Two machine learning models (DeepSphere and PointNet) have been used to evaluate the performance, using the waveform features as described before. The score obtained as a result of the machine learning for the first stage of the PID is shown in Figure 4.

The second step is more complicated, as neutrinos and anti-neutrinos have very similar features. However, their interactions may be distinguished using: i) Event kinematics, as neutrinos tend to transfer more energy to hadrons than antineutrinos, and ii) Secondary neutrons, since anti-neutrino interactions tend to produce more primary neutrons than neutrino interactions. The first is directly encoded in the waveform features of the primary trigger, already used. For the second, JUNO has the capability to identify and reconstruct the neutron triggers among the delayed signals following the interaction. This has been done adopting two different strategies. In Strategy 1, the interaction vertex

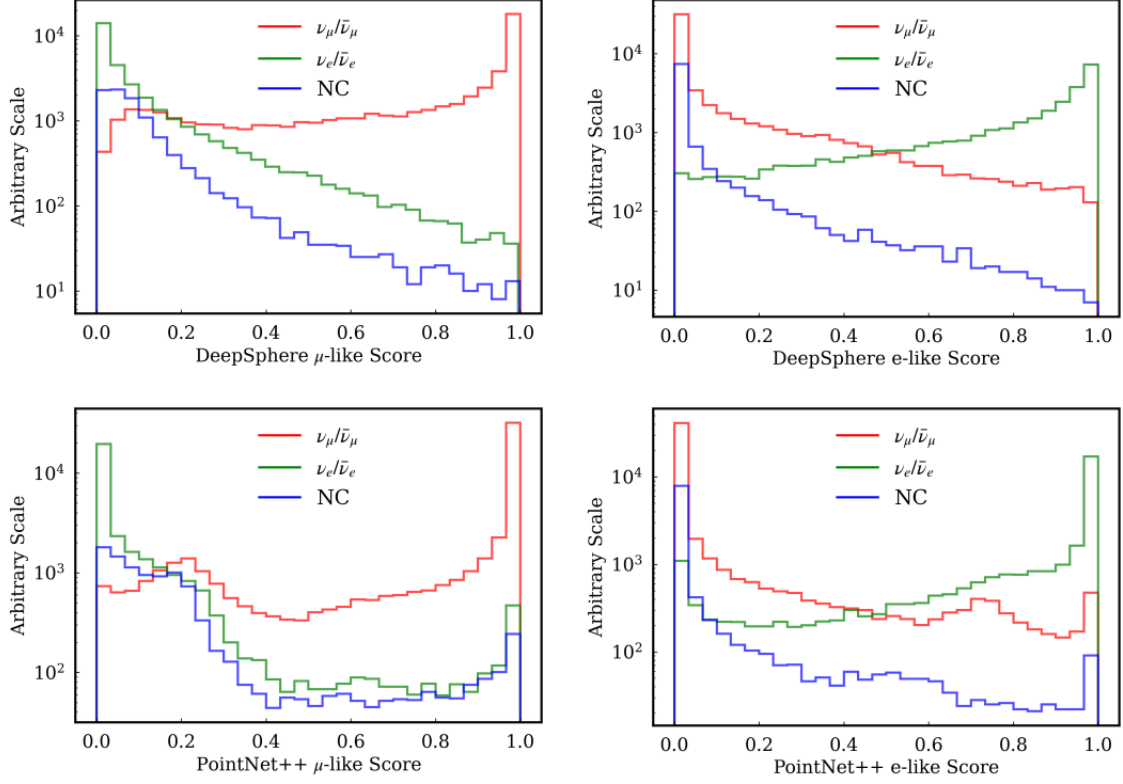


**Figure 4:** Distributions of the  $\mu$ -like score (left) and e-like score (right) by the Deepsphere (top) and PointNet++ (bottom) models. True  $\nu_\mu/\bar{\nu}_\mu$ -CC,  $\nu_e/\bar{\nu}_e$ -CC and NC events are shown in different colors. Figure extracted from [6].

from each delayed neutron-capture trigger is reconstructed and this information is incorporated to the training as a cloud of points. Strategy 2 merges the multiple neutron triggers into an one, with charge the sum of all neutron charges, and time, the time of the first selected neutron. The results of this second PID step are shown in Figure 5. We see that for muon flavor, a good separation between  $\nu_\mu$  and  $\bar{\nu}_\mu$  is achieved, while disentangling  $\nu_e$  and  $\bar{\nu}_e$  is more challenging.

## 6. Outlook and summary

This document summarizes the latest work done in the understanding of the detector response to GeV atmospheric neutrino interactions in JUNO, showing the potential for atmospheric neutrino studies with large liquid scintillator experiments. The final sensitivity results including this detector response and a full study of systematics on the way.

## References

- [1] A. Abusleme et al, JUNO Collaboration, Progr. Part. Nucl. Phys. 123 (2021) 103927
- [2] A. Abusleme et al, JUNO Collaboration, Chin.Phys.C 49 (2025) 3, 033104

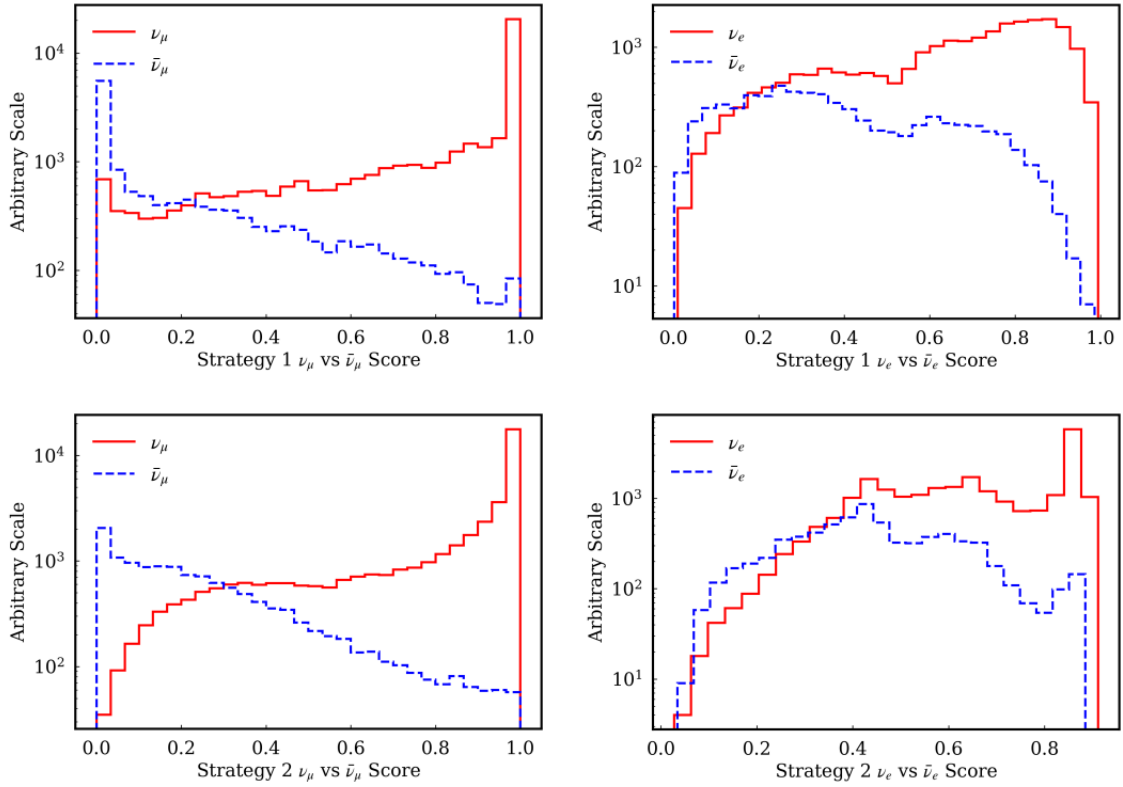


**Figure 5:** Left figures show the ML score result for  $\nu_\mu/\bar{\nu}_\mu$ -CC classification. Right figures, show the score obtained for the  $\nu_e/\bar{\nu}_e$ -CC separation. Top figures report the results for Strategy 1, while bottom Figures are drawn with the output of Strategy 2.

[3] K. Abe et al., Phys. Rev. D 97 (7 Apr. 2018), p. 072001

[4] C. Andreopoulos et al., "The GENIE Neutrino Monte Carlo Generator: Physics and User Manual", arXiv:1510.05494

[5] Z. Yang et al., Phys. Rev. D 109 (2024) 5, 052005

[6] J.iaxi Lu et al., "Neutrino type identification for atmospheric neutrinos in a large homogeneous liquid scintillation detector", arXiv:2503.21353